Smart Structures and Systems, *Vol. 31*, *No. 5* (*2023*) *531-543*
https://doi.org/10.12989/sss.2023.31.5.531

Self-centering passive base isolation system incorporating shape memory alloy wires for reduction in base drift

Sania Dawood [1a], Muhammad Usman[*1], Mati Ullah Shah [1b] and Muhammad Rizwan [2c]

[1] *School of Civil and Environmental Engineering* (*SCEE*), *National University of Sciences and Technology* (*NUST*), *H-12 Sector Islamabad 44000*, *Pakistan*
[2] *Military College of Engineering (MCE), National University of Sciences and Technology (NUST), Risalpur, KPK 24080, Pakistan*

(*Received July 27*, *2022*, *Revised March 24*, *2023*, *Accepted April 28*, *2023*)

Abstract. Base isolation is one of the most widely implemented and well-known technique to reduce structural vibration and damages during an earthquake. However, while the base-isolated structure reduces storey drift significantly, it also increases the base drifts causing many practical problems. This study proposes the use of Shape Memory Alloys (SMA) wires for the reduction in base drift while controlling the overall structure vibrations. A multi-degree-of-freedom (MDOF) structure along with base isolators and Shape-Memory-Alloys (SMA) wires in diagonal is tested experimentally and analytically. The isolation bearing considered in this study consists of laminates of steel and silicon rubber. The performance of the proposed structure is evaluated and studied under different loadings including harmonic loading and seismic excitation. To assess the seismic performance of the proposed structure, shake table tests are conducted on base-isolated MDOF frame structure incorporating SMA wires, which is subjected to incremental harmonic and historic seismic loadings. Root mean square acceleration, displacement and drift are analyzed and discussed in detail for each story. To better understand the structure response, the percentage reduction of displacement is also determined for each story. The result shows that the reduction in the response of the proposed structure is much better than conventional base-isolated structure.

Keywords: Multi-Degree of freedom (MDOF); passive base isolators; seismic response; self-centering; shake table testing; shape memory alloys

1. Introduction

An earthquake is one of the most terrifying natural disasters that humans cannot control as it causes maximum damage to life and buildings, especially multi-story buildings which are prone to destruction by earthquakes (Jose *et al*. 2021, Memon *et al*. 2020). Different traditional techniques i.e., increasing the dimensions of structural members (beams and columns) to strengthen the structure have been in use for a long period. A structure designed by this technique may survive an earthquake but may lead to a higher cost of building which is not efficient (Fan *et al*. 1991). To overcome the drawbacks of the traditional techniques many vibration control measures have been studied over recent years (Usman and Jung 2015, Tanveer *et al*. 2020). Base isolation is one of the most widely implemented and well-known techniques to reduce structural vibration and damages during an earthquake (Johnson *et al*. 1998, Arslan Hafeez *et al*. 2020). Presently base isolation is adopted all over the world as a reliable technique in earthquake designs of buildings. The concept of base isolation is to decouple a structure from earthquake ground movement by providing an isolation device that separates super-structure from the sub-structures (Ramallo *et al*. 2003). Using this technique in high-rise buildings, the deformation or distortion of superstructures can be dramatically reduced as the base isolation technique mitigate/lower the vibrations of earthquake transferring to the superstructure (Huang *et al*. 2014). Main isolation control systems are passive control, active control, and semi-active control systems (Shah and Usman 2022, Shah *et al*. 2022a, b). In addition, dampers can be used with an isolation system to attain vibration reduction within the system (Tanveer *et al*. 2019, Khan *et al*. 2021, Shah and Usman 2022, Huang *et al*. 2014). Several types of isolation devices are in use today including; Natural rubber bearings, high-damping rubber bearings, lead-Plug bearings, laminated rubber bearings, and frictional/sliding bearings (Baker 2007). Natural rubber bearing has two steel end plates (top & bottom) and multilayer thin rubber sheets bonded onto multi-layer thin steel shims. Lead rubber bearing is similar to silicon rubber bearing except for the lead core that supplies extra stiffness to the isolators. Similarly, laminated rubber bearings are made from high-purity elastomer (Bhatt *et al*. 2018). Researchers have introduced the use of smart materials as isolator elements to reduce vibrations and noise (Wang *et al*. 2020a).

SMA is a class of smart materials that offer unique characteristics of undergoing large reversible inelastic

*Corresponding author, Tenured Associate Professor,
E-mail: m.usman@nice.nust.edu.pk
[a] Graduate Student
[b] Graduate Student
[c] Associate Professor

ISSN: 1738-1584 (Print), 1738-1991 (Online)

deformation and enhancing the performance of various structures subjected to earthquakes (Varughese and El-Hacha 2020). SMAs are capable of recovering their pre-defined shape after experiencing and undergoing large strain (Varughese and El-Hacha 2020). SMAs undergo a phase transition that will occur between the high-temperature phase, austenite, and a low-temperature phase, martensite (Li *et al*. 2018). Due to these material features, SMAs are very effective in civil engineering applications (Liu *et al*. 2019).

Regarding the use of SMAs in isolation systems a significant amount of research has been done previously and reported in the literature. Wang (Wang *et al*. 2020b) investigated the damping effect and seismic behavior of SMA using the unit-cell finite element method. Varughese and El-Hacha (2020) investigated the natural behavior of the frames strengthened with NiTi shape memory alloy wires. Shi (Shi *et al*. 2020) studied the seismic performance of shape memory alloy (SMA) braced steel frame while considering the consequences of numerous design parameters and the ultimate state of smart material which is shape memory alloy. Yan and Wang (Yan *et al*. 2013) studied the mechanical properties of shape memory alloys (SMAs) wires along with SMA wire cable to actively lessen or mitigate dynamic responses of frame structure under earthquake excitations. Han (Han *et al*. 2003) investigated the effect of SMAs wires by installing SMAs dampers in a frame structure. An innovative copper aluminum beryllium wire-based sliding rubber bearing base isolator is presented and studied by Zheng and Bi (Zheng *et al*. 2021b) for earthquake protection of civil structure in cold areas. A unique re-centering seismic isolator (RSI) incorporating damping enhanced (DE) sliding lead rubber bearing (LRB) with super elastic shape has been designed by Zheng (Zheng *et al*. 2022c) to improve the bridge resilience performance. Zheng (Zheng *et al*. 2022a) has also demonstrated the benefits of superelastic sliding-LRB by comparing its performance with SMA-based friction pendulum bearing. Pang (Pang *et al*. 2021) presented a unique seismic risk-based methodology for an optimized design of SMA-restrained sliding bearings for highway bridges subject to near-fault ground vibrations. Zheng (Zheng *et al*. 2022b) presented a novel multi-stage superelastic variable stiffness pendulum isolator (SVSPI) incorporating SMA to improve the resilient capability of bridges. Fang (Fang *et al*. 2022) studied a novel type of shape memory alloy (SMA) cable-restrained high damping rubber (SMA-HDR) bearing particularly well suited to near-fault (NF) zones where the pulsing effect in the ground motions exist. Liang (Liang *et al*. 2020) introduced an innovative type of friction sliding bearing system incorporating SMA cables which outclassed the conventional sliding bearing system and steel-cable-control bearing system in terms of performance. Deng (Deng *et al*. 2022) experimentally verified that multi-level SMA-lead rubber-bearing isolation systems exhibit excellent re-centering capabilities.

Qiu and Zhu (2017) studied self-centering steel frames with innovative shape memory alloy braces (SMAB), which use super elastic Ni-Ti wires. Design and experimental study using SMA-based devices for the control of civil infrastructure proposed by Song and Li (Song *et al*. 2006). Omori (2012) investigated the application of Cu-Al-Mn super-elastic alloy (SEA) bar as a damping element in a frame structure by conducting shaking table tests. Dizaji (Dizaji and Dizaji 2021) proposed and evaluated a superplastic memory alloy re-centering damper system for enhancing and improving the performance of steel frame structures that have been exposed to several levels of seismic excitations and earthquake movements. Desroches and Smith studied the basic properties of shape memory alloys, focusing on the factors affecting their response and highlights the potential, as well as the limitations of the material for the seismic ground motion applications (Desroches and Smith 2004).

Zheng studied the SMA-based friction pendulum system for the vibration control of bridges and presented that SMA-based friction pendulum systems have reliable recentering and energy dissipation mechanisms for the bridges under near fault earthquakes (Zheng *et al*. 2021a). Li (Li *et al*. 2022) proposed a novel SMA wires-based roller bearing for reducing the over-displacement of the isolators and improving their self-centering mechanism having almost negligible residual deformation. Zheng (Zheng *et al*. 2023) proposed a novel superelastic isolator with multi-stage variable curvature for the vibration control of structures in cold regions. Wang (Wang *et al*. 2023) proposed a novel base isolation system consisting of conventional lead rubber bearing and superelastic SMA wires to improve the seismic resilience of important and strategic infrastructures. Zheng (Zheng *et al*. 2020) coupled sliding lead rubber bearings with superelastic SMA wires for better vibration control performance of continuous bridges. Gur (Gur *et al*. 2017) proposed a thermally modulated SMA friction pendulum to improve the base isolation system performance. Wang (Wang *et al*. 2020a) conducted an experimental study for understanding the behavior of SMA-based U-dampers in case of in-plane and out of plan loading conditions.Osman (Ozbulut and Hurlebaus 2011) investigated novel superelactic friction isolator for the bridges.

Liu and Van Humbeeck studied a critical heat treatment process for deformed NiTi SMAs to obtain a high martensite damping capacity (Liu and Van Humbeeck 1997). DesRoches studied the characteristics of super elastic Ni-Ti shape memory alloys under periodic loading to evaluate the capacity for applications in earthquake design (DesRoches *et al*. 2004). Qianhua Kan reported the effect of strain rate on the cyclic deformation of a super-elastic NiTi shape memory alloy (SMA) (Casciati and Marzi 2010). Spencer (Spencer *et al*. 2017) considered a cross-wire configuration for SMA wires and investigated the effect of the wires on high-damping rubber bearings (HDRB). Jani (Jani *et al*. 2014) describes the attributes of SMAs that make them ideally suited to actuators in various applications and provides a timely review of recent SMA research and commercial applications. A multi-level SMA/lead rubber bearing (ML-SLRB) isolation system was proposed by Cao (Cao *et al*. 2020) to ensure both isolation efficiency and capability to limit excessive bearing displacements under different levels of earthquake

excitations. The optimal performance of SMA-LRB isolated buildings under random earthquakes has been investigated by Masanobu Shinozuka (Shinozuka *et al*. 2015) to study the reduction of isolator displacement and resulting penalty of increased superstructure accelerations. A comprehensive experimental investigation of the mechanical properties of SMA wires under different numbers of cycles and strain amplitudes conducted by Zhang (Zhang *et al*. 2021). Dezfuli (Dezfuli and Alam 2013) studied SMA straight wires and cross wires configurations around the base isolator. In cross wires configuration there is a significant reduction in SMA wire strain, but this type of arrangement cannot operate in a super elastic range at large shear strain amplitude, especially when the height of the rubber bearing is increased Hedayati Dezfuli (Dezfuli *et al*. 2017) also studied SMA wires in double cross arrangement around the base isolator.

sA series of research efforts have been made by the researchers to utilize SMA wires as an important component of the isolation system. SMA wires in different configurations such as straight wires arrangement, cross wires arrangement, and double cross wires arrangement around the based isolator, have been investigated. It is important to note that in cross and double-cross arrangements the SMA wires studied in previous literature with the isolator are in the single plane. Moreover, arrangements in the literature, are only tested with a single isolator prototype without any structure level testing. Effect of SMA wires incorporation with multiple base isolators on the structural vibrations has not been explored. The significance and the novelty of the current study lies in the effect of SMA wires with two base isolators in a cross diagonal non-coplaner arrangement on vibrations of an MDOF structure.

The proposed system consists of a conventional isolated structure with SMA wires provided in a diagonal arrangement at the base level to reduce the base drift. The base isolation system studied consists of two laminated silicon rubber-bearing base isolators. The Nitinol SMA wires were provided in a diagonal arrangement. Several variations of SMA materials (Cu-Zn, Fe-Mn-Al-Ni, etc) were reviewed from the literature, however, NiTi wire was used owing to its high performance and better ductility (Huang *et al*. 2020). To assess the effects of the proposed system a series of shake table tests were conducted with different applied loadings (harmonic and earthquake excitations) and the results were discussed in detail. The structural vibration response of each story against all loadings was analyzed and compared with the conventional system. Power spectral density (PSD) curves against each loading for both proposed and conventional structures have also been compared and discussed in detail. The experimental results confirm the significant reduction in the base drift while showing effecting vibration reduction by using the proposed structure in a comparison of the conventional isolation systems.

2. Experimental study

2.1 Design of base isolators

The isolation system studied is a combination of two passive base isolators along with NiTi SMA wires in a diagonal. The primary parameter considered for the design of an adaptive base isolator is the vertical load-carrying capacity of the base isolation system. The loading capacity of the adaptive isolator depends on rubber material property (stiffness), shape factor effective area, and maximum strain of natural rubber therefore, an optimal design of base isolator is required for the proposed structure (Li *et al*. 2013).

The weight capacity of the adaptive base isolator is calculated by the following equations

$$\mathbf{W = A.G.S.}\gamma_w \tag{1}$$

In this equation, **'A'** is the area of the isolator which is the overlap of the top and bottom of the base isolator, the shear modulus of rubber is **G** and **S** is the shape factor of the rubber layer while γ_w is the allowable shear strain due to weight.

$$\mathbf{S = \phi/4t} \tag{2}$$

where **S** is the shape factor for a circular base isolator and ϕ is the diameter and **t** is the thickness of the circular plate. The horizontal stiffness of the passive base isolator is simplified as

$$\mathbf{K_b = GA/h} \tag{3}$$

From the above expressions, it can be observed that in the design of base isolators low horizontal stiffness can be achieved if the cross-sectional area of a laminated structure decreases or the thickness of the rubber layer increases. If the cross-sectional area of the isolator is not sufficient or the rubber layer is too thick, the isolator may become unsteady or unstable when subjected to seismic excitations. Therefore, an optimization of the parameters must be considered to retain the stability and enhance the effectiveness of the adaptive passive base isolator. The final assumed design parameters while considering the stability and performance of the base isolator have been shown in Table 1.

Table 1 Structural design parameters of passive base isolator

Parameters	NRBs
Area of base isolator	6388 mm
Weight capacity of base isolator	50 kg
Shape factor	12.5
Stiffness of base isolator	1870 N/m
Diameter of round rubber sheet	100 mm
Rubber layer thickness	2 mm
Number of rubber sheets	14
Total thickness of rubber sheets	28 mm

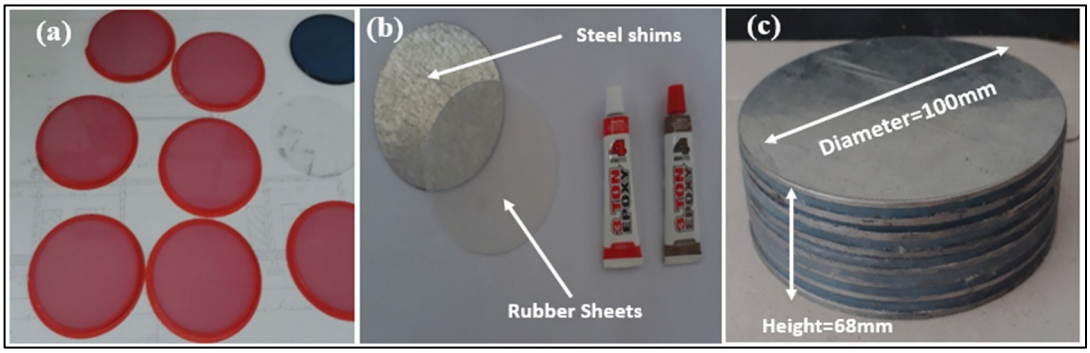

Fig. 1 (a) Moulding of silicone rubber layers in 3D printed moulds; (b) Steel and rubber layers along with the epoxy used; (c) Prepared laminated Rubber Bearing

Table 2 Dynamic and geometric properties of steel frame

Structural parameters			Modal properties	
Story level	**Mass (kg)**	**Stiffness (N/m)**	**Mode**	**Natural frequency (Hz)**
1	6.25	4444.5	First	1.89
2	6.25	4444.5	Second	5.29
3	6.25	4444.5	Third	7.64
Geometric properties of steel frame				
Weight of Steel Frame			32 kg	
Length of column			225 mm	
Length of beam			375mm	
Column Size			75mm x 2mm	
Beam Size			75mm x 8mm	
Base Plate size			875mm x 875mm x 35mm	

2.2 Fabrication of base isolators

Passive base isolators generally have two steel end plates (top and bottom) and multi-layer thin rubber sheets bonded onto multi-layer thin steel shims. The material used to fabricate rubber sheets was silicon rubber (RTV1505-A and RTV1505-B). The fabrication procedure of the sample consisted of mixing, molding & curing. The mold used for casting silicon rubber elastomers was made from polylactic acid (PLA) filament. PLA is probably the most widely available and popular filament used in 3D printing as it can be printed at a low temperature. To fabricate elastomers first, 50% of part A (RTV1505-A) and part B (RTV1505-B) of silicon rubber was added to a beaker and mixed manually. Then the sample was poured into a mold (100 mm diameter, 2 mm thickness) for curing. The curing time for the sample was 4-5 hours.

The material used for steel shims fabrication was galvanized iron sheets. Holes were drilled on the top and bottom plates of the base isolators to fix the isolators to the frame structure and on the shake table as well.

2.3 Test structure

Based on the discussion in section 2.1 above, an experimental model of the frame has been designed and fabricated. The design parameters of the frame are based on the stiffness and weight of the base isolator. The experimental model has been adopted from Bin Huang that was fabricated in the Smart Materials and Structures Laboratory at the university of Huouston (Huang *et al.* 2014).

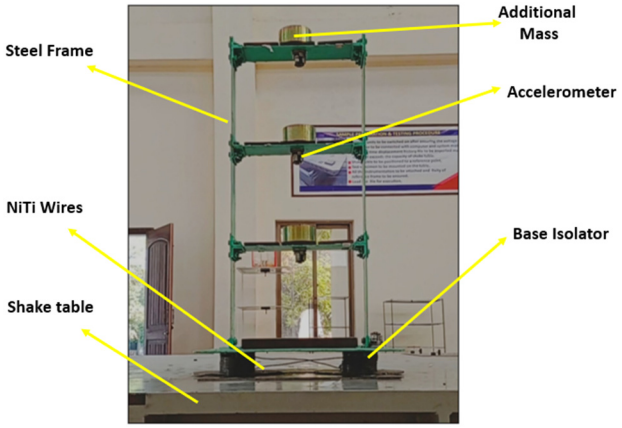

Fig. 2 (a) Moulding of silicone rubber layers in 3D printed moulds; (b) Steel and rubber layers along with the epoxy used; (c) Prepared laminated Rubber Bearing

The test setup used in this study was a 3-story steel frame that has been fabricated from galvanized iron sheet. As seen in Fig. 2 each story of the experimental model has

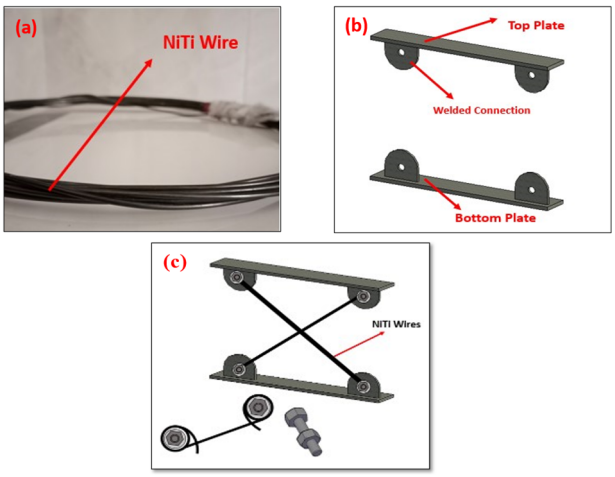

Fig. 3 (a) NiTi SMA Wire sample; (b) Top and Bottom plates fabricated to hold the SMA wires; (c) Diagonal arrangement for SMA wires

the same height, mass, and stiffness. The length of the beam and column for each story was 15 and 12 inches respectively. The width of the beam and column was 3 inches.

The parameters including mass, stiffness, and natural frequency presented in Table 2.

2.4 Provision of NiTi SMA wires

Nitinol Shape Memory Alloys offer unique characteristics of undergoing large reversible inelastic deformation and enhance the performance of various structures subjected to earthquakes. These wires experience deformation at one temperature and regain their earliest shape when heated above their transformation temperature. Due to high performance and good ductility, NiTi wires gained wide popularity in commercial applications.

In this study, NiTi wires (diameter = 3 mm) were used. The chemical composition of Nickel-titanium SMA wire is Nickel 55-56% and Titanium 44-45%. Fig. 3 shows the NiTi wire used in the proposed structure. Bolted connections were used to anchor the end of the SMA wire with welded connections. Nitinol is very erosion resistant and has self-centering properties. It does not require any special handling or protection from moisture and is non-toxic. However, the cost of this material may be a major barrier. Therefore, a suitable solution is to utilize SMA in a selected region of the structure.

2.4.1 AMOUNT OF SMA WIRE

Since, Ni-Ti based alloys show an extremely good shape memory effect, but the cost of this material is a major barrier. The amount of SMA wire mounted within the structures depends on whether they are used to prevent large deformations of structures or out of plan collapse of building. Other parameters to decide amount of SMAs are base drift and mass of Structure. In this study, the following steps were followed for the calculation of the amount of SMA wire:

- First, the diagonal length (L) of the wire between two base isolators was calculated.
- Then the maximum allowable base drift (**Δ**) in the structure was decided based on previous literature (Li *et al*. 2013).
- Required cross-sectional area (A) of the SMA wire was calculated using Hook's law.

$$\boldsymbol{A = \frac{PL}{E\delta}} \tag{4}$$

Here P is the allowable load, δ is the allowable elongation of the SMA wire and E is the elastic modulus of the SMA wire.

- Finally the diameter of the SMA wire was calculated using the area calculated in the previous step.

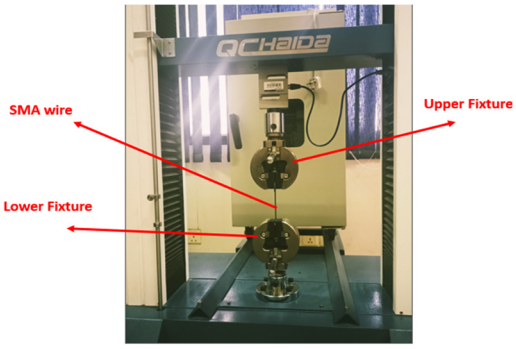

Fig. 4 Experimental Setup including SMA wire Specimen

2.4.2 Material characterization

The 3 mm diameter Nickel Titanium SMA wire used in the test was manufactured by BAOJI ZHONGYU RARE METALS CO., LTD. (Baoji, Shaanxi, China). Table 3 shows the mechanical properties of SMA wire specimen.

The testing of SMA wire was carried out using the universal testing machine at the National University of Science and Technology Islamabad. The test setup was composed of different parts, such as the sensor, upper fixture, lower fixture, and SMA wire as shown in Fig. 4. The gauge length of the wire in the test setup was 90 mm which corresponds to the distance between the upper and lower fixture. The load and displacements of the test

Table 3 Mechanical properties of SMA wire specimen

Alloy	Alloy	Content (%)		Diameter	Mass density	Tensile strength	Elongation
		Ni	Ti	(mm)	(kg/m^3)	(MPa)	(%)
Given	Nickel Titanium	55-56	45-46	3	6450	895	25-50
Experimental	-	-	-	-	6450	854.5	38.8

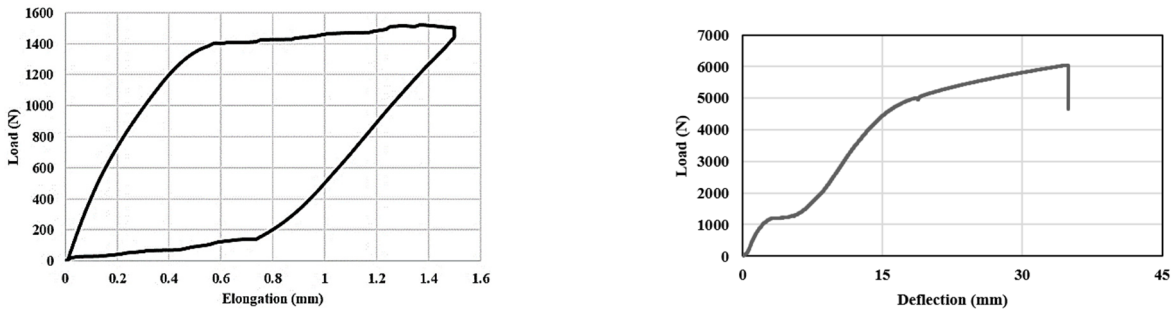

(a) (b)

Fig. 5 (a) Hysteresis loop for SMA wire; (b) load-deformation curve of SMA wire

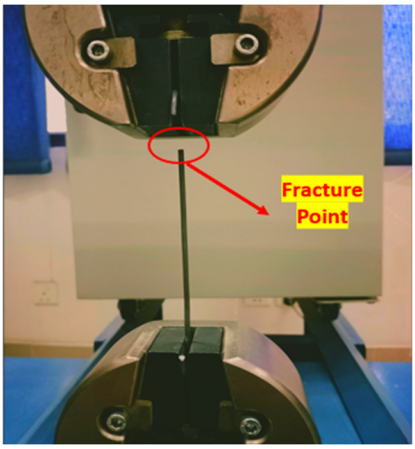

Fig. 6 Rupture of SMA wire specimen

specimens were directly recorded by test sensors. All the tests were conducted at room temperature (approximately 20-25°C).

The test was performed to study the behavior of the SMA wire. The specimen wire was tested at a loading rate of 3 mm/min. Fig. 5(a) shows the hysteresis loop of SMA wire under cyclic loading till 1.5 mm. The results show that the superelastic SMA wires have a stable mechanical yield point and sustained force performance after yielding. At unloading the wire restored its original shape without any residual deformation.

Fig. 5(b) shows the load-deflection curve for a wire specimen till fracture point. From the curve, it can be observed that at the start SMA wire shows a linear elastic behavior than a point reached where the wire begins to yield (marks the beginning of plastic deformation). The deflection of 38.46 mm in the curve is the point where a complete rupture occurred in SMA wire. The maximum stress and strain obtained against this deflection are 854.5 MPa and 38.8% respectively. Fig. 6 shows the rupture of SMA wire specimen.

Since the proposed structure was designed against 25% strain. From the curve it can be observed that the wire is not failed against the design drift of the structure and is falling well in the plastic range.

2.5 Experimental procedure

The entire setup for this study included a steel frame, passive base isolators, SMA wires, accelerometers and a Basmak shake table.

A series of shake table tests were conducted on the proposed system to establish experimental validation of the proposed system. Fig. 7 shows the schematic view of the

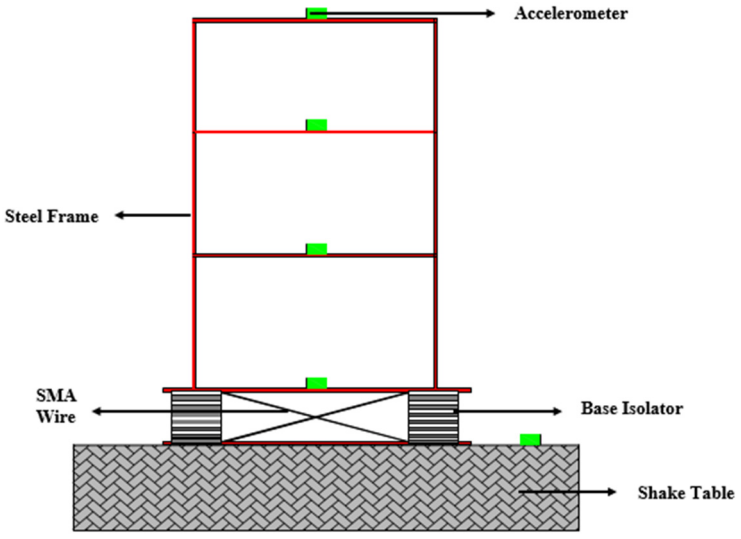

Fig. 7 Schematic view of the test setup

Table 4 Different test cases considered for the shake table testing

Cases:			
With wires		**Without wires**	
Harmonic loading			
Frequency (Hz)	**Four cases amplitude (mm)**	**Frequency (Hz)**	**Four cases amplitude (mm)**
0.5	5, 10, 15, 20	0.5	5, 10, 15, 20
1	5, 10, 15, 20	1	5, 10, 15, 20
1.5	5, 10, 15, 20	1.5	5, 10, 15, 20
2	5, 10, 15, 20	2	5, 10, 15, 20
HISTORIC LOADING			
EI Centro earthquake loading			

proposed system. The wireless accelerometer nodes were attached on each DOF of the steel frame structure and on the top of the shake table to record the acceleration data during a variety of external loads. The accelerometer nodes used in this study can record the accelerations up to a sampling rate of 256 Hz. The data recorded from this accelerometer is in the form of a CSV file. The experiments have been performed on the uniaxial shake table in a structural dynamic laboratory of the Military College of Engineering (MCE-NUST) Risalpur. The shake table used in testing has a maximum payload of 15 tons. The acceleration capacity of the table is ±2 g. The loading applied was harmonic and earthquake excitation.

Harmonic loadings including frequencies of 0.5 Hz, 1 Hz, 1.5 Hz, and 2 Hz were applied. These loadings were applied at different amplitudes including 5 mm, 10 mm, and 15 mm. These excitations were feasible to assess the

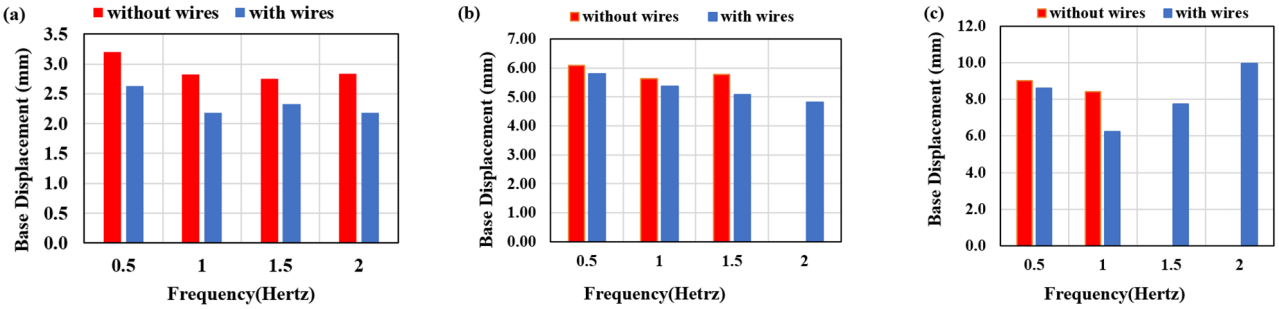

Fig. 8 Base displacements against frequencies for different amplitudes: (a) Amplitude 5 mm; (b) Amplitude 10 mm; (c) Amplitude 15 mm

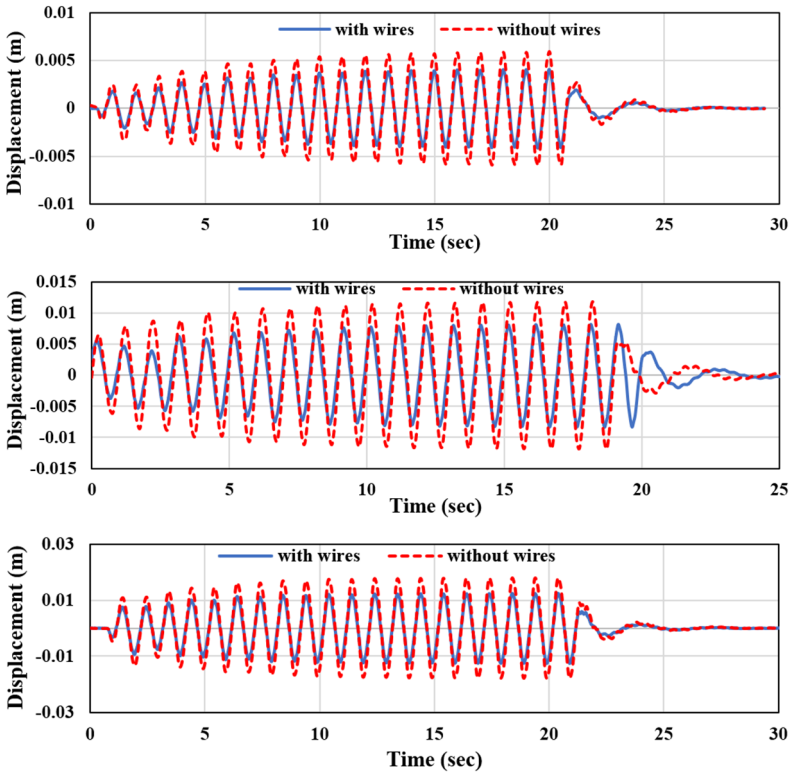

Fig. 9 Base displacement-time graphs of proposed & conventional structure including loadings of 1 Hz: (a) Amplitude 5 mm; (b) Amplitude 10 mm; (c) Amplitude 15 mm

effectiveness of the proposed structure (base isolators along with wires) and the conventional structure (base isolators without wires). In earthquake excitation, the loading applied was El Centro. At first, two identical superelastic SMA wires were attached to base isolators, and then harmonic loading was applied to the structure, including 0.5 Hz, 1 Hz, 1.5 Hz, and 2 Hz at an amplitude of 5 mm. The tests were repeated for 10 mm and 15 mm amplitudes respectively to study the effects of SMA wires on the damping properties of the proposed structure.

The acceleration data was recorded from accelerometers and stored in the form of CSV files. Finally, the EI Centro earthquake excitation was applied by the shake table. The seismic excitation loading was applied for both proposed and conventional system. The accelerometers on each story record acceleration data for both cases against all loading conditions. From accelerations data, the maximum relative displacements and story drifts were obtained for the proposed system. To compare the results, same calculations were implemented and analyzed for the conventional system.

3. Results and discussions

3.1 Displacement response to harmonic loading

The acceleration response for both cases (with wires & without wires) has been recorded for all stories. The response values indicate the vibration of the structure for all loading conditions. For analysis, the displacement response for both structures have been calculated and compared. In all loadings, the results show that the story drift of the proposed structure reduced as compared to that of the conventional structure. In the proposed structure the SMA wires used is NiTi which is very effective for base isolation as it has a strong ability of energy dissipation and recentering. To compare and analyze the results, the story drift response has been calculated for both proposed and conventional systems.

3.1.1 Base displacement response

Fig. 8 shows the base displacement response for both structures. The response has been observed for loading on the structures including 0.5 Hz, 1 Hz, 1.5 Hz, and 2 Hz with a varying amplitude of 5 mm, 10 mm, and 15 mm respectively. Part (a) in the figure shows the response at an amplitude of 5 mm. Similarly, Part (b) and Part (c) show the response of the base for 10mm and 15mm amplitude. The SMA wires used in the proposed system can reduce the base drift.

From Fig. 8 it has been observed that the RMS base displacement response of the proposed structure was reduced as compared to the conventional structure. For all loading proposed structure show maximum reduction as compared to the conventional system. Part (a) in the figure shows a reduction against 0.5 Hz. For 1 Hz and 2 Hz, the reduction is almost the same while base displacement reduction against 1.5 Hz is the maximum. In part (b) maximum displacement reduction has been observed against 1.5 Hz, while for 2 Hz only the proposed structure displacement has been shown because the conventional system (without wires) failed at this loading condition. Similarly in part(c) base displacement reduction has been observed but for loading conditions of 1.5 Hz and 2 Hz just the proposed structure response has shown as the conventional system already failed against this loading.

Fig. 9 shows the displacement response of the base for both structures. The response has been observed for loading of 1 Hz with a varying amplitude of 5 mm, 10 mm, and 15 mm respectively. Part (a) in the figure shows the response at an amplitude of 5 mm. Similarly, Part (b) and Part (c) show the response of the base for 10 mm and 15 mm amplitude. The proposed structure displacement response has been compared with the conventional structure response.

From Fig. 9 it has been observed that the displacement of the proposed structure is reduced as compared to the conventional structure. For all varying amplitudes proposed structure shows a maximum reduction in displacement as compared to a conventional system.

3.1.2 Story drift response

The story drift response for both cases (with wires & without wires) has been calculated and compared in this section. Fig. 10 shows the RMS story drift response of both structures. The response has been observed for loading on the structures including 0.5 Hz, 1 Hz, 1.5 Hz, and 2 Hz with a varying amplitude of 5 mm, 10 mm, and 15 mm respectively. In all stories proposed structure shows a reduction in drift against each loading. In Fig. 10 part (a)

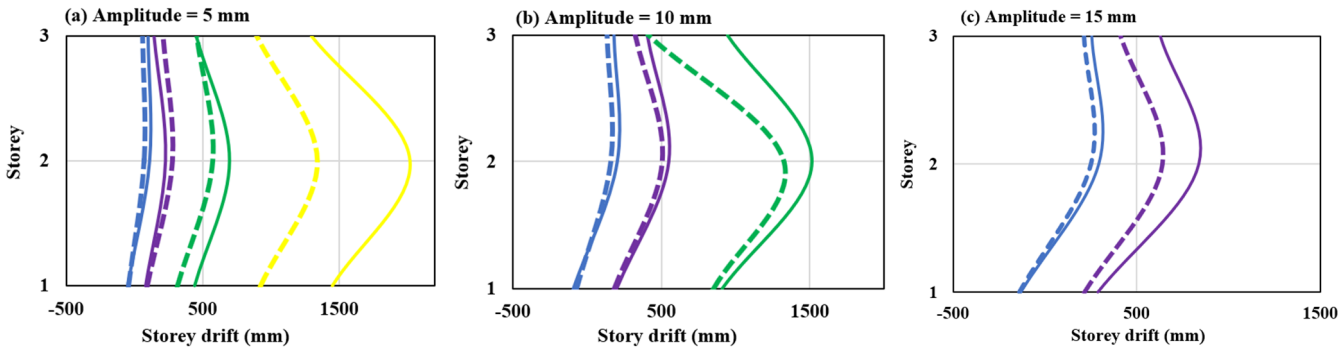

Fig. 10 RMS storey drift response of proposed and conventional structure for different amplitudes: (a) Amplitude 5 mm; (b) Amplitude 10 mm; (c) Amplitude 15 mm

Table 5 Percentage reduction in the drift response of with wire over without wire

	Amplitude = 5 mm			Amplitude = 10 mm			Amplitude = 15 mm	
Storey level	**0.5 Hz**	**1 Hz**	**1.5 Hz**	**0.5 Hz**	**1 Hz**	**1.5 Hz**	**0.5 Hz**	**1 Hz**
Base	**49.93**	**59.26**	**55.57**	**44.71**	**45.18**	**17.00**	**33.22**	**46.07**
1	8.089	11.27	28.26	-4.16	0.099	0.165	-4.864	25.594
2	36.12	17.18	17.56	20.24	7.97	12.47	15.16	23.84
3	40.60	30.47	0.794	24.44	19.50	56.25	17.22	34.59

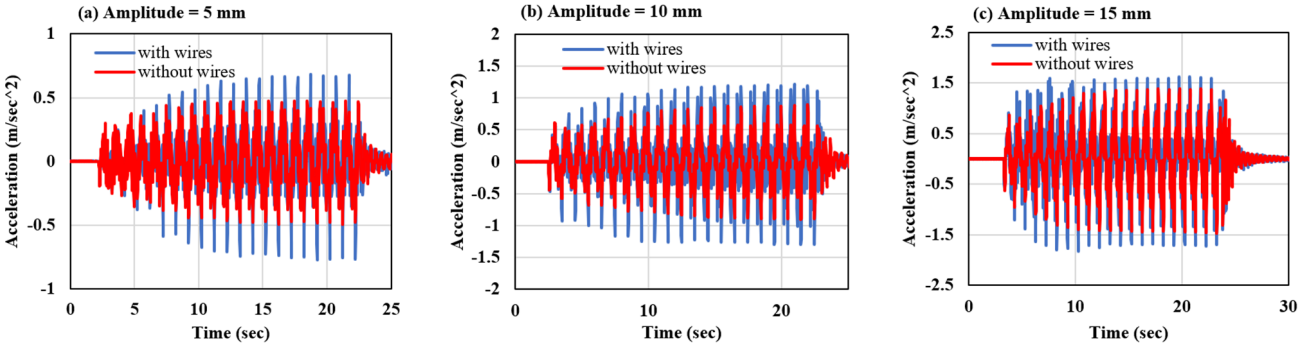

Fig. 11 Base acceleration Time histories of proposed & conventional structure including loadings of 1 Hz: (a) Amplitude 5 mm; (b) Amplitude 10 mm; (c) Amplitude 15 mm

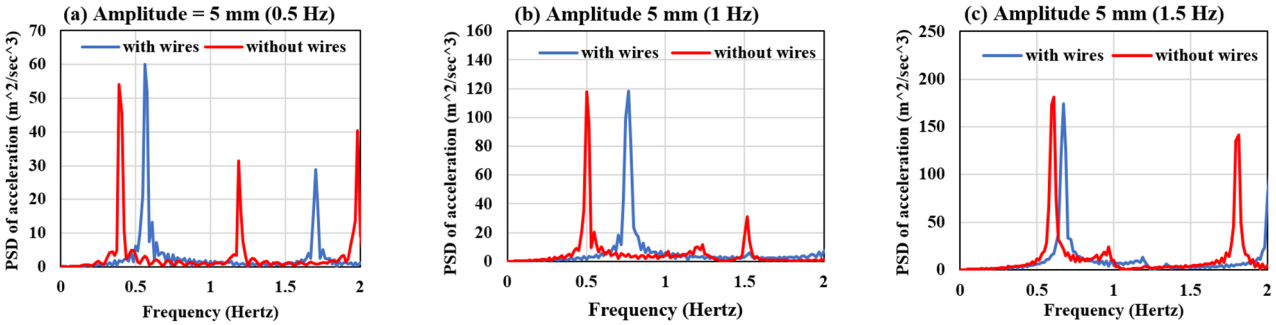

Fig. 12 PSD Response for harmonic loading: (a) 0.5 Hz; (b) 1 Hz; (c) 1.5 Hz

a small reduction in the drift of each story has been observed for a loading condition of 0.5 Hz and 1 Hz, while for 1.5 Hz and 2 Hz, a large reduction of drift in each story has been observed. Similarly, in part (b) and part (c) of Fig. 10, drift reduction has been observed in each story for all loading conditions.

Fig. 10 shows that with the increase in frequency, the drift reduction is more visible in the proposed structure. The effect of the SMA wire used in the proposed structure is more profound at higher frequencies, due to which the story drift or structural displacements does not produce any significant effect on the structure at low frequencies.

Fig. 12 shows the response of the proposed structure in the frequency domain. The power spectral density response has been investigated for all input loading conditions. Fig. 12 part(a) shows the PSD response for the loading condition of 0.5 Hz. Part(b) and (c) show the PSD response against 1 Hz and 1.5 Hz loadings respectively. From Fig. 12 it has been observed that peaks of PSD ordinates have been suppressed and shifted in the forward direction.The shift of peak in the forward direction is due to an increase in accelerations of proposed structure. Based on the discussion in section 3.2 as the drift decrease the accelerations at the base level increases which is inline with the reported literature (Wilde *et al*. 2000).

3.3 Response to EI Centro loading

Fig. 13 shows the time histories of the EI Centro earthquake for both proposed and conventional structures. Since there is no response reduction in the proposed structure due to a sudden increase in accelerations. This is due to the fact reported by Krzysztof Wilde, that adding dampers to the isolation system results in an increase in the acceleration response (Wilde *et al*. 2000).

3.3 Response to EI Centro loading

Fig. 13 shows the time histories of the EI Centro earthquake for both proposed and conventional structures.

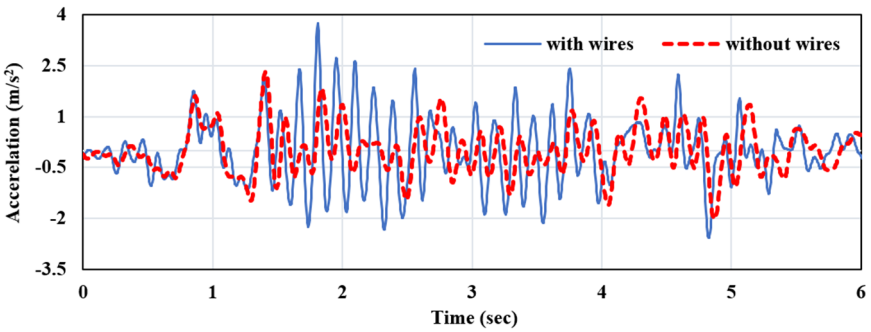

Fig. 13 Base acceleration-time histories against earthquake loading: EI Centro

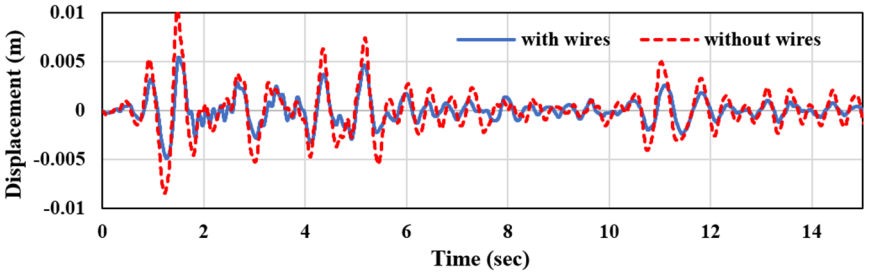

Fig. 14 Base displacement-time graphs against earthquake loading: EI Centro

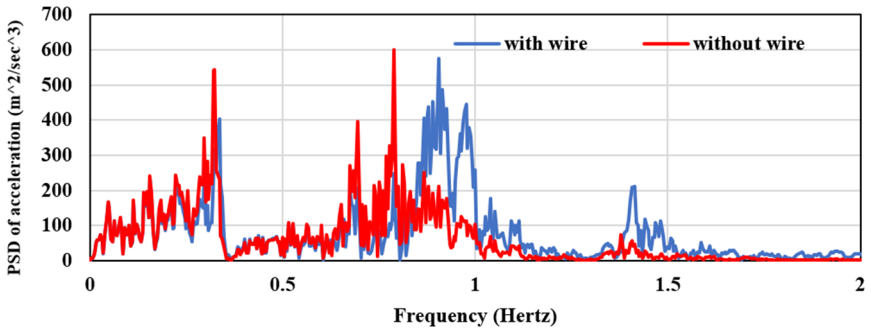

Fig. 15 PSD Response for base acceleration when subjected to EI Centro earthquake loadings

Since there is no response reduction in the proposed structure due to a sudden increase in accelerations. This is due to the fact reported by Krzysztof Wilde, that adding dampers to the isolation system results in an increase in the acceleration response (Wilde *et al*. 2000).

Fig. 15 shows the PSD curves against EI Centro earthquake loading. The peaks have been observed between 0.5 Hz and 1 Hz. The peak has been suppressed significantly in the proposed structure and shifted towards a higher frequency.

The shift towards higher frequency is due to an increase in the accelerations of the proposed structure. Koo reported that adding dampers to the isolation system results in an increase in the acceleration response (Koo *et al*. 2021), which is in line with the observations on this study.

4. Conclusions

In this study, a multi-degree-of-freedom structure along with base isolators and SMA wires in a diagonal is proposed. For the performance optimization, experimental model was fabricated and tested in a structural dynamic laboratory of the Military College of Engineering (MCE-NUST) Risalpur. The performance of the proposed structure was studied for both harmonic loading and seismic excitations.

From the experimental investigation, it was illustrated that

- Incorporation of SMA wires in passive base isolation system showed promising results by significantly reducing base drift in addition to reduction in story drift.
- Base Drift in case of harmonic loading was reduced up to 59 % compared to conventional structure.
- Story drifts were reduced up to 41 % compared to the conventional structure.
- A frequency shift was observed due to the application of SMA wire which is in line with previous literature.
- Consequently, the acceleration magnitude was

slightly increased which was expected due to the frequency shift.

This study effectively demonstrates that the proposed SMA isolation system possesses the ability of energy dissipation as well the capability of recovering the original shape which is very suitable for a structure subjected to earthquakes. However, for future studies, the effect of the proposed system needs investigation when subjected to different characteristic earthquakes.

References

Arslan Hafeez, M., Usman, M., Umer, M.A. and Hanif, A. (2020), "Recent progress in isotropic magnetorheological elastomers and their properties: A Review", *Polymers*, **12**(12), 3023. https://doi.org/10.3390/polym12123023

Baker, J.W. (2007), "Measuring bias in structural response caused by ground motion scaling", *Proceedings of Pacific Conference on Earthquake Engineering*, no. 056, pp. 1-6. https://doi.org/10.1002/eqe

Bhatt, G., Paul, D.K. and Bhowmick, S. (2018), "Design of Base Isolation System for Buildings", In: *Design and Optimization of Mechanical Engineering Products*, pp. 67-82. https://doi.org/10.4018/978-1-5225-3401-3.ch004

Cao, S., Ozbulut, O.E., Wu, S., Sun, Z. and Deng, J. (2020), "Multi-level SMA/lead rubber bearing isolation system for seismic protection of bridges", *Smart Mater. Struct.*, **29**(5), p. 055045. https://doi.org/10.1088/1361-665X/ab802b

Casciati, S. and Marzi, A. (2010), "Experimental studies on the fatigue life of shape memory alloy bars", *Smart Struct. Syst., Int. J.*, **6**(1), 73-85. https://doi.org/10.12989/sss.2010.6.1.073

Deng, J., Hu, F., Ozbulut, O.E. and Cao, S. (2022), "Verification of multi-level SMA/lead rubber bearing isolation system for seismic protection of bridges", *Soil Dyn. Earthq. Eng.*, **161**, 107380. https://doi.org/10.1016/j.soildyn.2022.107380

DesRoches, R. and Smith, B. (2004), "Shape memory alloys in seismic resistant design and retrofit: a critical review of their potential and limitations", *J. Earthq. Eng.*, **8**(3), 415-429. https://doi.org/10.1080/13632460409350495

DesRoches, R., McCormick, J. and Delemont, M. (2004), "Cyclic properties of superelastic shape memory alloy wires and bars", *J. Struct. Eng.*, **130**(1), 38-46. https://doi.org/10.1061/(asce)0733-9445(2004)130:1(38)

Dezfuli, F.H. and Alam, M.S. (2013), "Shape memory alloy wire-based smart natural rubber bearing", *Smart Mater. Struct.*, **22**(4), 045013. https://doi.org/10.1088/0964-1726/22/4/045013

Dezfuli, F.H., Li, S., Alam, M.S. and Wang, J.Q. (2017), "Effect of constitutive models on the seismic response of an SMA-LRB isolated highway bridge", *Eng. Struct.*, **148**, 113-125. https://doi.org/10.1016/j.engstruct.2017.06.036

Dizaji, F.S. and Dizaji, M.S. (2021), "A Novel Smart Memory Alloy Re-Centering Damper for Passive Protection of Structures Subjected to Seismic Excitations Using High-Performance NiTiHfPd Material", (ArXiv:2105.04081v1 [Nlin.AO]), ArXiv Adaptation and Self-Organizing Systems 22901.

Fan, F.G., Ahmadi, G., Mostaghel, N. and Tadjbakhsh, I.G. (1991), "Performance analysis of aseismic base isolation systems for a multi-story building", *Soil Dyn. Earthq. Eng.*, **10**(3), 152-171. https://doi.org/10.1016/0267-7261(91)90029-Y

Fang, C., Liang, D., Zheng, Y. and Lu, S. (2022), "Seismic performance of bridges with novel SMA cable-restrained high damping rubber bearings against near-fault ground motions", *Earthq. Eng. Struct. Dyn.*, **51**(1), 44-65. https://doi.org/10.1002/eqe.3555

Gur, S., Frantziskonis, G.N. and Mishra, S.K. (2017), "Thermally modulated shape memory alloy friction pendulum (tmSMA-FP) for substantial near-fault earthquake structure protection", *Struct. Control Health Monitor.*, **24**(11), e2021. https://doi.org/https://doi.org/10.1002/stc.2021

Han, Y.L., Li, Q.S., Li, A.Q., Leung, A.Y.T. and Lin, P.H. (2003), "Structural vibration control by shape memory alloy damper", *Earthq. Eng. Struct. Dyn.*, **32**(3), 483-494. https://doi.org/10.1002/eqe.243

Huang, B., Zhang, H., Wang, H. and Song, G. (2014), "Passive base isolation with superelastic nitinol SMA helical springs", *Smart Mater. Struct.*, **23**(6), p. 065009. https://doi.org/10.1088/0964-1726/23/6/065009

Huang, H., Zhu, Y.Z. and Chang, W.S. (2020), "Comparison of bending fatigue of NiTi and CuAlMn shape memory alloy bars", *Adv. Mater. Sci. Eng.*, **2020**, 1-9. https://doi.org/10.1155/2020/8024803.

Jani, J.M., Leary, M., Subic, A. and Gibson, M.A. (2014), "A review of shape memory alloy research, applications and opportunities", *Mater. Des.*, **56**, 1078-1113. https://doi.org/10.1016/j.matdes.2013.11.084

Johnson, Erik A, Juan C Ramallo, Billie F Spencer, and Michael K Sain. (1998), "Intelligent base isolation systems", *Proceedings of the Second World Conference on Structural Control*, Kyoto, Japan, June-July, pp. 1-10.

Jose, S.K., Anjali, G.S., Nair, A.S., Adithya, D.A., Sony, A. and Arunima, A.S. (2021), "Fixed and Base Isolated Framed Structures: A Comparative Study", *J. Phys.: Conference Series*, **2070**(1). https://doi.org/10.1088/1742-6596/2070/1/012198

Khan, I.U., Usman, M. and Tanveer, M. (2021), "Vibration control of an irregular structure using single and multiple tuned mass dampers", *Proceedings of the Institution of Civil Engineers - Structures and Buildings*, **12**, 1-26. https://doi.org/10.1680/jstbu.21.00011

Komur, M., Karabork, T. and Deneme, I. (2011), "Nonlinear dynamic analysis of isolated and fixed-base reinforced concrete structures", *Gazi Univ. J. Sci.*, **24**(3), 463-475.

Koo, G.H., Shin, T.M. and Ma, S.J. (2021), "Shaking table tests of lead inserted small-sized laminated rubber bearing for nuclear component seismic isolation", *Appl. Sci.*, **11**(10), p. 4431. https://doi.org/10.3390/app11104431

Li, J., Li, Y., Li, W. and Samali, B. (2013), "Development of adaptive seismic isolators for ultimate seismic protection of civil structures", *Proceedings of Sensors and Smart Structures Technologies for Civil, Mechanical, and Aerospace Systems*, Vol. 8692, San Diego, CA, USA, March. https://doi.org/10.1117/12.2009626

Li, H.N., Liu, M.M. and Fu, X. (2018), "An innovative re-centering SMA-lead damper and its application to steel frame structures", *Smart Mater. Struct.*, **27**(7), p. 075029. https://doi.org/10.1088/1361-665X/aac28f.

Li, S., Dezfuli, F.H., Alam, M.S. and Wang, J.Q. (2022), "Design, manufacturing, and performance evaluation of a novel smart roller bearing equipped with shape memory alloy wires", *Smart Mater. Struct.*, **31**(2), 25032. https://doi.org/10.1088/1361-665X/ac4690

Liang, D., Zheng, Y., Fang, C., Yam, M.C. and Zhang, C. (2020), "Shape memory alloy (SMA)-cable-controlled sliding bearings: Development, testing, and system behavior", *Smart Materials and Structures*, **29**(8), 85006. https://doi.org/10.1088/1361-665X/ab8f68

Liu, Y. and J. Van Humbeeck. (1997), "On the damping behaviour of NiTi shape memory alloy", *Le Journal de Physique IV*, **7**(5), C5-519. https://doi.org/10.1051/jp4:1997582

Liu, Y., Wang, H., Qiu, C. and Zhao, X. (2019), "Seismic behavior of superelastic shape memory alloy spring in base isolation system of multi-story steel frame", *Materials*, **12**(6), p. 997.

https://doi.org/10.3390/ma12060997
Memon, S.A., Zain, M., Zhang, D., Rehman, S.K.U., Usman, M. and Lee, D. (2020), "Emerging trends in the growth of structural systems for tall buildings", *J. Struct. Integr. Maint.*, **5**(3), 155-170. https://doi.org/10.1080/24705314.2020.1765270
Omori, T. (2012), "Cu-Al-Mn Super-elastic Alloy Bars as Dissipative Brace System in Structural Steel Frame", *Proceedings of the 15th World Conference on Earthquake Engineering* (*15WCEE*).
Ozbulut, O.E. and Hurlebaus, S. (2011), "Optimal design of superelastic-friction base isolators for seismic protection of highway bridges against near-field earthquakes", *Earthq. Eng. Struct. Dyn.*, **40**(3), 273-291. https://doi.org/https://doi.org/10.1002/eqe.1022
Pang, Y., He, W. and Zhong, J. (2021), "Risk-based design and optimization of shape memory alloy restrained sliding bearings for highway bridges under near-fault ground motions", *Engineering Structures*, **241**, 112421. https://doi.org/10.1016/j.engstruct.2021.112421
Qiu, C. and Zhu, S. (2017), "Shake table test and numerical study of self-centering steel frame with SMA braces", *Earthq. Eng. Struct. Dy.*, **46**(1), 117-137. https://doi.org/10.1002/eqe.2777
Ramallo, J.C., Johnson, E.A., Spencer, B.F. and Sain, M.K. (2003), "Semi-active building base isolation", *Proceedings of the 1999 American Control Conference* (*Cat. No. 99CH36251*), San Diego, CA, USA. https://doi.org/10.1109/acc.1999.782881
Shah, M.U. and Usman, M. (2022), "An experimental study of tuned liquid column damper controlled multi-degree of freedom structure subject to harmonic and seismic excitations", *Plos one*, **17**(6), e0269910. https://doi.org/10.1371/journal.pone.0269910
Shah, M.U., Usman, M., Farooq, S.H. and Kim, I.H. (2022a), "Effect of tuned spring on vibration control performance of modified liquid column ball damper", *Appl. Sci.*, **12**(1), 318. https://doi.org/10.3390/app12010318
Shah, M.U., Usman, M., Farooq, S.H. and Rizwan, M. (2022b), "Spring-controlled modified tuned liquid column ball damper for vibration mitigation of structures", *J. Sound Vib.*, **545**, p. 117443. https://doi.org/10.1016/j.jsv.2022.117443
Shi, F., Ozbulut, O.E. and Zhou, Y. (2020), "Influence of shape memory alloy brace design parameters on seismic performance of self-centering steel frame buildings", *Struct. Control Health Monitor.*, **27**(1), 1-18. https://doi.org/10.1002/stc.2462
Shinozuka, M., Chaudhuri, S.R. and Mishra, S.K. (2015), "Shape-memory-alloy supplemented lead rubber bearing (SMA-LRB) for seismic isolation", *Probabil. Eng. Mech.*, **41**, 34-45. https://doi.org/10.1016/j.probengmech.2015.04.004
Song, G., Ma, N. and Li, H.N. (2006), "Applications of shape memory alloys in civil structures", *Eng. Struct.*, **28**(9), 1266-1274. https://doi.org/10.1016/j.engstruct.2005.12.010
Spencer, K., Hedayati Dezfuli, F. and Alam, M. (2017), "Design and Performance Evaluation of Shape Memory Alloy (SMA) Cross-Wire Configured High Damping Rubber Bearing", In: *Leadership in Sustainable Infrastructure*, pp. 1-10, Canadian Society for Civil Engineering; Vancouver, Canada.
Tanveer, M., Usman, M., Khan, I.U., Ahmad, S., Hanif, A. and Farooq, S.H. (2019), "Application of tuned liquid column ball damper (TLCBD) for improved vibration control performance of multi-storey structure", *PLoS One*, **14**(10), 1-15. https://doi.org/10.1371/journal.pone.0224436
Tanveer, M., Usman, M., Khan, I.U., Farooq, S.H. and Hanif, A. (2020), "Material optimization of tuned liquid column ball damper (TLCBD) for the vibration control of multi-storey structure using various liquid and ball densities", *J. Build. Eng.*, **32**, 101742. https://doi.org/https://doi.org/10.1016/j.jobe.2020.101742
Ullah, M., Usman, M., Kim, I.H. and Dawood, S. (2022), "Analytical and experimental investigations on the performance of tuned liquid column ball damper considering a hollow ball", *Struct. Eng. Mech., Int. J.*, **83**(5), 655-669. https://doi.org/10.12989/sem.2022.83.5.655
Usman, M. and Jung, H.J. (2015), "Recent developments of magneto-rheological elastomers for civil engineering applications", *Smart Material Actuators: Recent Advances in Material Characterization and Application*, Hauppauge, NY, USA.
Varughese, K. and El-Hacha, R. (2020), "Design and behaviour of steel braced frame reinforced with NiTi SMA wires", *Eng. Struct.*, **212**, 110502. https://doi.org/10.1016/j.engstruct.2020.110502
Wang, B., Zhu, S. and Casciati, F. (2020a), "Experimental study of novel self-centering seismic base isolators incorporating superelastic shape memory alloys", *J. Struct. Eng.*, **146**(7), 4020129. https://doi.org/10.1061/(ASCE)ST.1943-541X.0002679
Wang, J., Cao, Y., Xu, Y., Gu, X., Zhu, J. and Zhang, W. (2020b), "Finite element modeling of the damping capacity and vibration behavior of cellular shape memory alloy", *Mech. Adv. Mater. Struct.*, **29**(15), 2142-2155. https://doi.org/10.1080/15376494.2020.1852349
Wang, B., Chen, P., Zhu, S. and Dai, K. (2023), "Seismic performance of buildings with novel self-centering base isolation system for earthquake resilience", *Earthq. Eng. Struct. Dyn.*, **52**(5), 1360-1380. https://doi.org/https://doi.org/10.1002/eqe.3820
Wilde, K., Gardoni, P. and Fujino, Y. (2000), "Base isolation system with shape memory alloy device for elevated highway bridges", *Eng. Struct.*, **22**(3), 222-229. https://doi.org/10.1016/S0141-0296(98)00097-2
Yan, S., Niu, J., Mao, P., Song, G. and Wang, W. (2013), "Experimental research on passive control of steel frame structure using SMA wires", *Mathe. Problems Eng.*, 2013. https://doi.org/10.1155/2013/416282
Zhang, B., Zeng, S., Tang, F., Hu, S., Zhou, Q. and Jia, Y. (2021), "Experimental and Numerical Analysis of the Mechanical Properties of a Pretreated Shape Memory Alloy Wire in a Self-Centering Steel Brace", *Processes*, **9**(1), 1-15. https://doi.org/10.3390/pr9010080
Zheng, W., Wang, H., Li, J. and Shen, H. (2020), "Parametric study of superelastic-sliding LRB system for seismic response control of continuous bridges", *J. Bridge Eng.*, **25**(9), 4020062. https://doi.org/10.1061/(ASCE)BE.1943-5592.0001596
Zheng, W.Z., Wang, H., Li, J. and Shen, H.J. (2021a), "Parametric study of SMA-based friction pendulum system for response control of bridges under near-fault ground motions", *J. Earthq. Eng.*, **25**(8), 1494-1512. https://doi.org/10.1080/13632469.2019.1582442
Zheng, W., Wang, H., Hao, H. and Bi, K. (2021b), "Superelastic CuAlBe wire-based sliding lead rubber bearings for seismic isolation of bridges in cold regions", *Eng. Struct.*, **247**, 113102. https://doi.org/10.1016/j.engstruct.2021.113102
Zheng, W., Tan, P., Li, J., Wang, H., Tan, J. and Sun, Z. (2022a), "Sliding-LRB incorporating superelastic SMA for seismic protection of bridges under near-fault earthquakes: A comparative study", *Soil Dyn. Earthq. Eng.*, **155**, 107161. https://doi.org/10.1016/j.soildyn.2022.107161
Zheng, W., Tan, P., Liu, Y., Wang, H. and Chen, H. (2022b), "Multi-stage superelastic variable stiffness pendulum isolation system for seismic response control of bridges under near-fault earthquakes", *Struct. Control Health Monitor.*, **29**(12), 1-17. https://doi.org/10.1002/stc.3114
Zheng, W., Tan, P., Zhang, Z., Wang, H. and Sun, Z. (2022c), "Damping enhanced novel re-centering seismic isolator incorporating superelastic SMA for response control of bridges under near-fault earthquakes", *Smart Mater. Struct.*, **31**(6), p.

065015. https://doi.org/10.1088/1361-665X/ac6b6a
Zheng, W., Tan, P., Li, J., Wang, H., Liu, Y. and Xian, Z. (2023), "Superelastic pendulum isolator with multi-stage variable curvature for seismic resilience enhancement of cold-regional bridges", *Eng. Struct.*, **284**, 115960. https://doi.org/https://doi.org/10.1016/j.engstruct.2023.115960

HJ